Journal of Applied Electrochemistry **31**: 1285–1291, 2001.

A spectroelectrochemical investigation of the influence of sodium diisobutyldithiophosphinate on silver dissolution in aqueous cyanide

G.A. HOPE, R. WOODS and K. WATLING
School of Science, Griffith University, Nathan, Queensland 4111, Australia

Received 19 April 2001; accepted in revised form 25 July 2001

Key words: corrosion inhibition, cyanide, diisobutyldithiophosphinate, flotation collector, Raman spectroscopy, silver

Abstract

Polarization studies have been carried out to determine the influence of diisobutyldithiophosphinate (DIBDTPI) on the dissolution of silver in cyanide solutions at pH 11. DIBDTPI was found to inhibit dissolution at concentrations similar to those used when this compound is applied as a flotation collector. The inhibition efficiency in 10^{-2} mol dm^{-3} CN^- was found to increase with increase in DIBDTPI concentration in the range 10^{-6}–10^{-4} mol dm^{-3}, and with increase in time of exposure of the silver to the DIBDTPI solution. The inhibition efficiency found for 10^{-4} mol dm^{-3} DIBDTPI in quiescent 10^{-2} mol dm^{-3} CN^- solution at 23 °C was 64.6% and 95.0% for exposure times of 10 min and 2 h, respectively. These values are significantly less than those found previously for 2-mercaptobenzothiazole under the same conditions. Surface enhanced Raman spectroscopy showed that inhibition was associated with adsorption of DIBDTPI displacing cyanide from the silver surface. Voltammetry at 0.5 mV s^{-1} indicated that adsorption of DIBDTPI involves charge transfer.

1. Introduction

In a recent publication [1] an electrochemical investigation was reported on the suppression of silver dissolution in alkaline cyanide solutions by 2-mercaptobenzothiazole (MBT). The objective of that study was to determine the extent to which a flotation collector could diminish silver losses in flotation when cyanide is used as a depressant. It was pointed out that, in the flotation separation and concentration of metal sulfides from lead/zinc ores, the lead component is recovered first, with the zinc often depressed by the addition of cyanide. Silver minerals are normally present as minor, but very valuable components of lead/zinc ores, and are recovered in the lead concentrate. Cyanide is a most effective leachant for the hydrometallurgical recovery of silver [2] and other precious metals from their ores. Hence, its use as a flotation depressant can result in loss of silver due to dissolution of silver minerals into the pulp as silver cyano-complexes. The extent of silver loss depends on the nature of the silver mineral and the flotation procedure adopted and it would appear advantageous if the collector used to recover the lead component also acted as a corrosion inhibitor for the silver content.

Diisobutyldithiophosphinate (DIBDTPI) was introduced in the late 1970s by Cytec Industries as a sulfide mineral flotation collector and is marketed as Aerophine promoter 3418A [3]. The structure of this collector is:

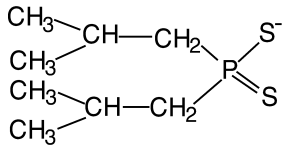

DIBDTPI has proved to be a particularly effective collector for the recovery of silver from complex base metal sulfide ores. It is a proficient collector for galena and hence is applied in the treatment of lead/zinc ores containing high silver values.

It was considered pertinent to determine the influence of DIBDTPI on the dissolution of silver in cyanide solution and compare the inhibition efficiency observed with that previously reported for MBT under the same conditions. The results of this study are presented and discussed in the present communication.

2. Experimental details

2.1. *Materials*

Electrodes were prepared from pure silver (Johnson Matthey 99.9%). A strip of surface area 1.32 cm^2 was used for triangular potential sweep voltammetry, polarization measurements and Raman spectroscopy. The

electrodes were abraded with P1200 silicon carbide paper wetted with doubly deionized water. Prior to the electrochemical experiments, the electrodes were sonicated with doubly deionized water for 2 min.

DIBDTPI was supplied by Cytec Industries as a 50% solution in aqueous alkali. This solution was acidified to precipitate DIBDTPI in its acid form and the compound recovered by filtration. The silver compound was obtained by dissolving the acid compound in NaOH, neutralising the solution, and adding $AgNO_3$ to precipitate AgDIBDTPI. Solid NaDIBDTPI was prepared by evaporating the water from the 50% solution in a vacuum desiccator.

Aqueous solutions of DIBDTPI for the corrosion studies were prepared from the acid form of the compound by dissolution in a carbonate/bicarbonate buffer solution of pH 11 prepared by mixing 0.034 mol dm^{-3} $NaHCO_3$ with 0.031 mol dm^{-3} NaOH. All reagents employed were of AR grade and solutions were prepared with doubly deionized water having a maximum conductivity of 0.030 μS cm^{-1}. High purity nitrogen (Linde 99.99%) was used for purging cells.

2.2. *Triangular potential sweep voltammetry and polarization curves*

Current–potential curves were recorded at 23 °C with an ADInstruments potentiostat controlled with a MacLab/4e unit and interfaced with a Macintosh computer operating with 'Echem' software. Potentials were measured against a Cypress Systems Ag/AgCl miniature reference electrode (electrolyte 3 mol dm^{-3} KCl) and converted to the standard hydrogen electrode (SHE) scale taking the potential of the Ag/AgCl electrode to be 0.21 V on the SHE scale. Polarization curves for silver dissolution were recorded with electrodes that had undergone corrosion in the solution of interest. The pretreatment procedure involved immersing a freshly prepared electrode in 50 ml of quiescent test solution in equilibrium with air for a selected period and the corrosion potential monitored with a MacLab/4e driven by ADInstruments 'Chart' software. The polarization scans were commenced at ~20 mV below the open circuit potential observed in the deaerated solution. Potential scans were run at 0.5 mV s^{-1}.

Polarization curves for oxygen reduction were determined in pH 11 buffer containing 0, 10^{-6}, 10^{-5} or 10^{-4} mol dm^{-3} DIBDTPI. Carrying out these investigations in the absence of cyanide allowed the potential region to be explored in which dissolution of silver to form cyano-complexes occurs. The potential was initially held at 0.5 V and then a scan applied in the negative-going direction at 0.25 mV s^{-1}.

Triangular potential sweep voltammograms were also recorded on the MacLab system for silver electrodes in the absence and presence of 10^{-3} mol dm^{-3} DIBDTPI.

2.3. *Surface enhanced Raman scattering (SERS) spectroscopy*

SERS spectra were obtained with a Renishaw RM2000 Raman spectrometer equipped with a computer controlled stage and a Leica metallurgical microscope incorporating a range of objectives. The FWHM of silicon calibration peak at 520 cm^{-1} was 5 cm^{-1} and the wavenumber resolution was 1 cm^{-1}. The incident radiation was conveyed from a Spectra Physics argon ion laser of 514.5 nm laser excitation, through a single mode fibre optic cable. A three-electrode electrochemical cell fitted onto the microscope stage and contained an optical window above the working electrode.

The silver electrode was heated in a furnace at 450 °C for 16 h to remove any contaminants from its surface and a SERS active surface was established by the application of three oxidation–reduction cycles between −0.2 and 0.6 V in 1 mol dm^{-3} KCl acidified with HCl, following an initial reduction period at −0.5 V. The electrode was then immersed in the cell containing pH 11 buffer solution together with 10^{-2} mol dm^{-3} CN^- and $l0^{-4}$ mol dm^{-3} DIBDTPI in equilibrium with air and spectra recorded *in situ* at the corrosion potential, using an ultra long working distance objective with 20× magnification. Since water is a weak Raman scatterer, the gap between the cell window and the electrode can be a few millimetres and hence there are no problems with mass transport limitation during *in situ* studies. SERS spectra were also recorded *in situ* at controlled potentials. Raman spectra were recorded for solid AgDIBDTPI and NaDIBDTPI using the same collection instrumentation with an objective of 50× magnification.

3. Results and discussion

3.1. *Polarization curves*

Polarization curves for the silver electrode in the pH 11 buffer solution containing 10^{-2} mol dm^{-3} CN^- in the absence of DIBDTPI and in the presence of 10^{-6}, 10^{-5} or 10^{-4} mol dm^{-3} of this organic species are presented in Figure 1 in the form of an Evans diagram. In each case, the electrode had been exposed for 10 min to a solution of the same composition in equilibrium with air prior to insertion into the cell. It can be seen that the presence of DIBDTPI at a concentration $\geqslant 10^{-5}$ mol dm^{-3} shifts the anodic polarization curve slightly to higher potentials.

The rest potential for a silver electrode in solutions in equilibrium with air (the corrosion potential, E_{corr}) and the values observed for solutions of the same composition as in Figure 1 are presented in Table 1. The corrosion current, i_{corr}, was obtained from the polarization curves in Figure 1; it was taken as the current flowing at a potential equal to the experimental value of E_{corr}. The table also presents the corrosion rate in μg m^{-2} s^{-1} and the inhibition efficiency (IE), expressed as a percentage, derived from the corrosion rates using the expression:

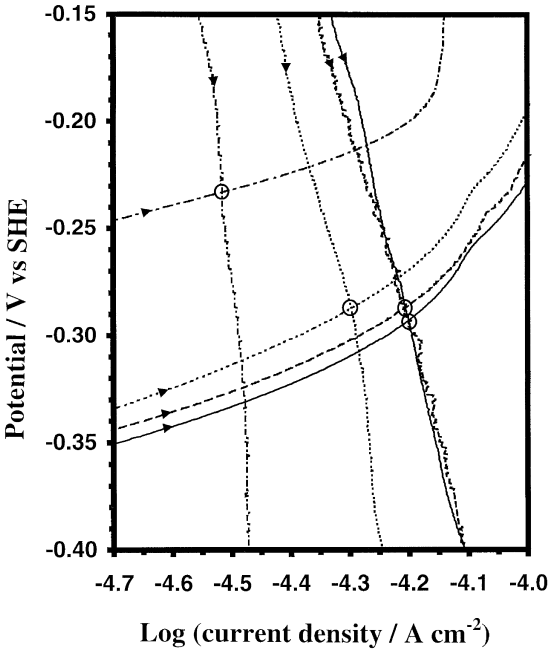

Fig. 1. Polarization curves for silver in pH 11 buffer solution containing (—) 0, (– – – –) 10^{-6}, (- - - -) 10^{-5} and (·····) 10^{-4} mol dm^{-3} DIBDTPI; arrows show the direction of the potential excursion. Negative-going scans are oxygen reduction currents in solution in equilibrium with air carried out at 0.25 mV s^{-1}; positive-going scans are silver dissolution currents in deoxygenated solution also containing 10^{-2} mol dm^{-3} CN^- carried out at 0.5 mV s^{-1}. Circles mark the intersection of the silver dissolution and oxygen curves for each DIBDTPI concentration.

Table 1. Corrosion rate and inhibition efficiency derived from the measured E_{corr} and anodic polarization curves

Exposure time	[DIBDTPI] /mol dm^{-3}	E_{corr} /V vs SHE	i_{corr} /μA cm^{-2}	Corrosion rate /μg m^{-2} s^{-1}	Inhibition efficiency /%
10 min	0	−0.295	61.4	686	–
	10^{-6}	−0.297	53.4	597	13.0
	10^{-5}	−0.292	46.7	522	23.9
	10^{-4}	−0.244	21.7	243	64.6
2 h	10^{-5}	−0.266	39.7	444	35.3
	10^{-4}	0.009	3.0	34	95.0

$$IE = \left(1 - \frac{r_s}{r_b}\right) \times 100 \quad (1)$$

where r_s and r_b are the corrosion rates in the presence and absence of DIBDTPI, respectively.

Figure 1 also shows cathodic polarization curves for oxygen reduction in pH 11 solutions containing the same range of DIBDTPI concentrations as was used to obtain the anodic, silver-dissolution curves. These solutions did not contain cyanide. It is apparent that the presence of DIBDTPI shifts the cathodic curves to more negative potentials and hence inhibits oxygen reduction as well as silver dissolution. Assuming that the presence of cyanide does not effect the oxygen reduction process, the intersection of the cathodic and anodic curves will correspond to the corrosion potential and the corrosion current for silver at each DIBDTPI concentration in cyanide solution in equilibrium with air.

The E_{corr} and i_{corr} values derived from Figure 1 are presented in Table 2 where they are compared with the data obtained from experimental E_{corr} values. As was found for analogous studies with MBT [1], the values obtained by the two approaches agree within experimental error and this validates the assumption that the presence of cyanide does not have a significant effect on the rate of oxygen reduction on a silver surface.

It is clear from Figure 1 that both silver dissolution and oxygen reduction are impeded by the presence of DIBDTPI, although the magnitude of the inhibition under these conditions is significantly less than that observed previously for MBT [1]. The interaction of DIBDTPI with silver was the subject of a voltammetric and *ex situ* infrared spectroelectrochemical study by Basilio et al. [4]. These authors observed the emergence of an IR spectrum indicating the deposition of Ag-DIBDTPI on the silver electrode surface after it had been treated at a potential of ~0.25 V in a solution of 2×10^{-4} mol dm^{-3} DIBDTPI and 0.05 mol dm^{-3} sodium tetraborate. The IR absorption intensity was found to increase with increase in potential above this value. No interaction between silver and DIBDTPI was reported at potentials below 0.2 V. Since the reversible potential of the Ag/AgDIBDTPI couple is independent of pH, the results of Basilio et al. indicate that the formation of AgDIBDTPI would not be expected below 0.2 V at pH 11. This potential is about half a volt higher than the region in which DIBDTPI was observed to influence the kinetics of reactions at the surface of a silver electrode in Figure 1.

To explore further the influence of DIBDTPI on silver dissolution in cyanide solutions, voltammograms were recorded in which the potential was scanned in the positive-going direction to higher values than those in Figure 1. As before, the electrodes were preconditioned in solutions of the same composition in equilibrium with air. The resulting voltammograms are presented in Figure 2 and they show that the inhibition of silver dissolution at a DIBDTPI concentration of 10^{-4} mol dm^{-3} becomes enhanced at potentials above −0.2 V. The curve for an electrode pretreated for 10 min in 10^{-4} mol dm^{-3} DIBDTPI shows that the silver surface

Table 2. Corrosion data derived from intersection of the polarization curves in Figure 1 compared with experimental values of E_{corr} and of i_{corr} at E_{corr} (Table 1)

[DIBDTPI] /mol dm^{-3}	From Figure 1		From Table 1	
	E_{corr} /V vs SHE	i_{corr} /μA cm^{-2}	E_{corr} /V vs SHE	i_{corr} /μA cm^{-2}
0	−0.294	61.7	−0.295	61.4
10^{-6}	−0.289	60.3	−0.297	53.4
10^{-5}	−0.288	50.1	−0.292	46.7
10^{-4}	−0.233	30.2	−0.244	21.7

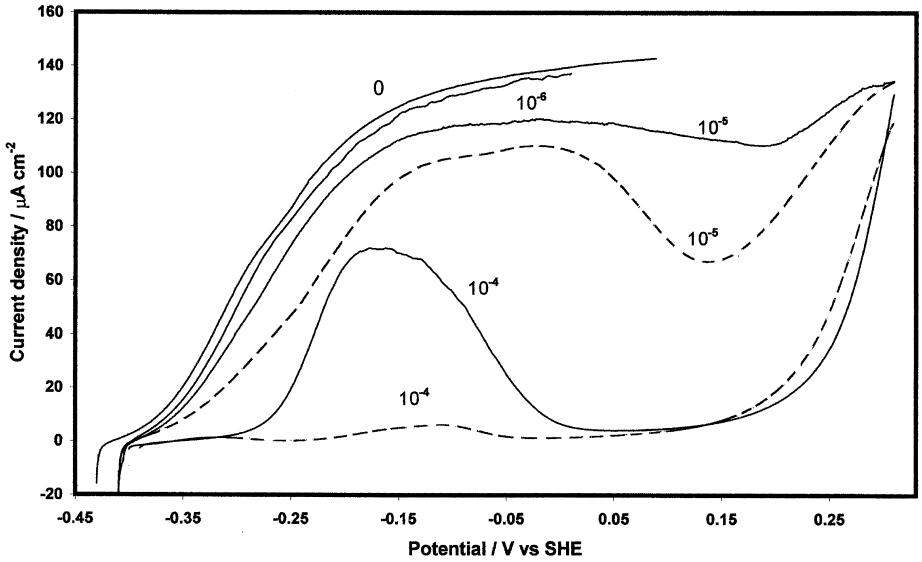

Fig. 2. Polarization curves at 0.5 mV s^{-1} in the positive-going direction for silver in deaerated solutions of the pH 11 buffer containing 10^{-2} mol dm^{-3} CN^- together with 0, 10^{-6}, 10^{-5} or 10^{-4} mol dm^{-3} DIBDTPI. Silver electrode immersed in a solution of the same composition in equilibrium with air for (—) 10 min and (– – – –) 2 h prior to transfer to the electrochemical cell.

became passive at ~0 V and remained in this condition until the potential was taken above 0.1 V. The potential then entered a transpassive region and the anodic current increased again. Polarization curves were also recorded on a potential scan at 5 mV s^{-1} for 10^{-4} mol dm^{-3} DIBDTPI. At this scan rate, no passive region was observed and this indicates that the formation of the inhibiting surface layer is a slow process.

Figure 2 includes polarization curves for a silver electrode that was pretreated in the test solution containing 10^{-5} or 10^{-4} mol dm^{-3} DIBDTPI in equilibrium with air for 2 h prior to transfer to the deaerated cell. It is apparent that the inhibition of silver dissolution increases with increase in exposure time. Table 1 presents the corrosion potentials observed for these two conditions and the corresponding corrosion rates. In the case of 10^{-4} mol dm^{-3} DIBDTPI, the corrosion potential was observed to increase over the first few minutes from about −0.3 V to about −0.24 V, then increase slowly for 1 h. After that period, the corrosion potential increased rapidly to ~0.05 V and remained at this value over the second hour. This behaviour can be explained by the inhibition of silver dissolution increasing with time until the peak current in the active region due to silver dissolution (see Figure 2) is less than that for oxygen reduction in the same potential region. This will force the potential through the passive into the transpassive region. At the higher potential, the oxygen reduction current is much smaller and hence the corrosion current much less. Under these conditions, the inhibition efficiency of DIBDTPI is significantly greater (Table 1) and becomes closer to that observed with MBT (Table 3).

The electrochemical findings could be explained by adsorption of DIBDTPI or an impurity compound present in the collector. In order to distinguish between these possibilities, spectroelectrochemical techniques are required. Raman spectroscopy is particularly useful for studying the interaction of collectors with the coinage metals [5] as a result of the sensitivity enhancement that is experienced with such surfaces and the fact that spectra can be recorded *in situ* in aqueous media.

Table 3. Comparison of inhibition efficiency observed for DIBDTPI and MBT

Exposure time	Collector concentration /mol dm^{-3}	Inhibition efficiency of DIBDTPI	Inhibition efficiency of MBT
10 min	10^{-6}	13.0	20.8
	10^{-5}	23.9	72.5
	10^{-4}	64.6	98.9
2 h	10^{-4}	95	99.4

3.2. *Surface enhanced Raman spectroscopy*

The Raman spectra of AgDIBDTPI and NaDIBDTPI are presented in Figure 3. The band at 531 cm^{-1} for NaDIBDTPI and that at 522 cm^{-1} for AgDIBDTPI can be assigned to the P–S stretching vibration [6]. Most of the other bands arise from vibrations within the isobutyl groups. The broad band at ~3400 cm^{-1} arises from vibrations of water of hydration associated with the sodium ion in the lattice. Figure 3 curve (a) is an *in situ* SERS spectrum obtained from a silver surface at the open circuit potential after 3 min exposure to a pH 11 solution containing 10^{-2} mol dm^{-3} CN^- together with 10^{-4} mol dm^{-3} DIBDTPI in equilibrium with air. The spectrum displays all the bands displayed by the silver and sodium DIBDTPI compounds and hence it can be concluded that the species present on the silver surface is DIBDTPI and not an impurity. The spectrum also displays a band at 2114 cm^{-1} which can confidently be

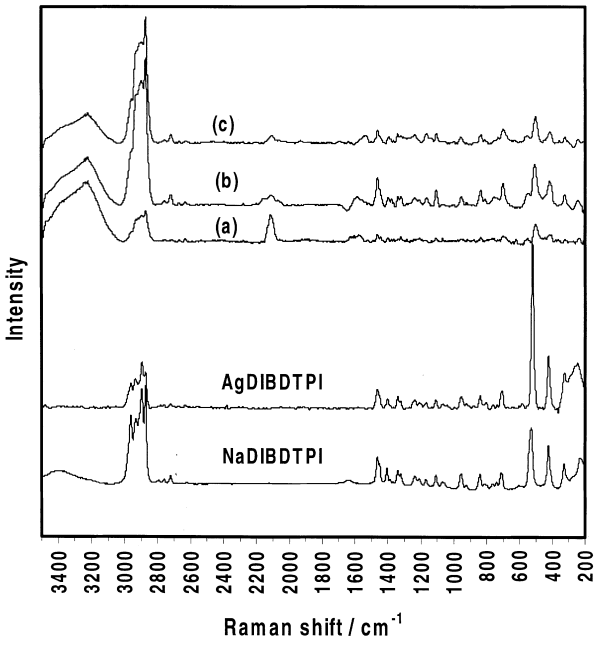

Fig. 3. Raman spectra for AgDIBDTPI and NaDIBDTPI and SERS spectra from a silver electrode in pH 11 solution containing 10^{-2} mol dm^{-3} CN^- together with 10^{-4} mol dm^{-3} DIBDTPI in equilibrium with air (a) at the open circuit potential; (b) then held at 0 V and (c) the potential finally decreased to −0.3 V.

assigned to the C≡N stretching vibration from cyanide bonded directly to silver atoms in the surface or to adsorbed silver cyano-complexes [1, 7].

Figure 3, curve (b) shows an *in situ* SERS spectrum from the same silver surface as for curve (a) after the potential had been increased to 0 V. It is apparent that the intensity of the bands arising from DIBDTPI are increased whereas that from cyanide is decreased. This is consistent with the observation from polarization curves that the inhibition of silver dissolution is enhanced at the higher potential. Curve (c) in Figure 3 is a SERS spectrum from the same silver electrode after the potential had been decreased again to −0.3 V, that is, close to the value of the corrosion potential. The intensity of each band is similar to those of the spectrum recorded at 0 V rather than that at the corrosion potential (curve (a)). Thus, the surface species responsible for corrosion inhibition is not formed reversibly.

Experiments were also carried out in which a SERS spectrum was recorded at 0 V and then the electrode immersed in doubly deionized water and sonicated. SERS spectra were subsequently recorded *ex situ*. It was found that the intensities of the bands arising from the stretching mode of cyanide were diminished significantly whereas those from DIBDTPI were similar to those in curve (b). This again shows that the adsorption of DIBDTPI is not reversible.

The band from the P–S stretching vibration in curves (a)–(c) appeared at 502, 509 and 501 cm^{-1}, respectively. This corresponds to a shift of 20, 13 and 21 cm^{-1} to lower wavenumbers from that for AgDIBDTPI. The other bands appeared at the same wavenumbers, within experimental error, as those for AgDIBDTPI. The shift could be due to a difference in the conformation of the chemisorbed radical to that in solid AgDIBDTPI. A shift of a similar magnitude was observed for the major band assigned to a NCS stretch vibration in the initial monolayer of MBT adsorbed on silver compared to that for AgMBT [8].

The above properties of the SERS spectra would indicate that the surface species present on the surface at the corrosion potential is formed by charge transfer adsorption:

$$DIBDTPI^- \rightarrow (DIBDTPI)_{ads} + e^- \qquad (2)$$

in which the adsorbed DIBDTPI in bonded to silver atoms in the surface through its two sulfur atoms. Raman spectroelectrochemical studies have shown that analogous mechanisms occur prior to the development of the metal-collector compound in the adsorption of ethyl xanthate on copper, silver and gold [9, 10], isoxanthates on silver [5, 11], *O*-isopropyl-*N*-ethylthionocarbamate [5, 12] and MBT on copper, silver and gold [5, 8].

3.3. *Triangular potential sweep voltammetry*

The voltammogram reported by Basilio et al. [4] for silver in DIBDTPI solutions did not display any significant current in the potential region close to −0.2 V. However, the voltammograms also failed to exhibit a current at the potential at which the IR intensity was observed arising from the formation of AgDIBDTPI. The voltammogram reported by those authors showed that silver oxide formation on the electrode was inhibited when DIBDTPI was present and from this behaviour it was inferred that AgDIBDTPI must have been present on the silver surface. The results reported here suggest that DIBDTPI adsorption is a slow process and hence the non-appearance of a voltammetric current could be due to the relatively rapid scan rate used by these authors (50 mV s^{-1}). Thus, voltammetry was carried out in the present work at slower scan rates.

A typical voltammogram obtained at 5 mV s^{-1} is shown in Figure 4(a). The supporting electrolyte was 0.05 mol dm^{-3} sodium tetraborate of pH 9.2, the same as in the work of Basilio et al.; this solution was used rather than that of pH 11 to enhance the separation between the formation of AgDIBDTPI and AgOH. This enhancement arises because the reversible potential of the former reaction is independent of pH while that of the latter shifts 59 mV to more positive potentials for each unit increase in pH. It can be seen from Figure 4 that, in the absence of DIBDTPI, an anodic current commences at a potential near the upper limit of the scan and this is due to the oxidation of silver to AgOH; a cathodic current arising from the reverse process occurs at the beginning of the return scan. Cathodic current is apparent at the lower limit on both negative and positive-going scans as a result of hydrogen evolution.

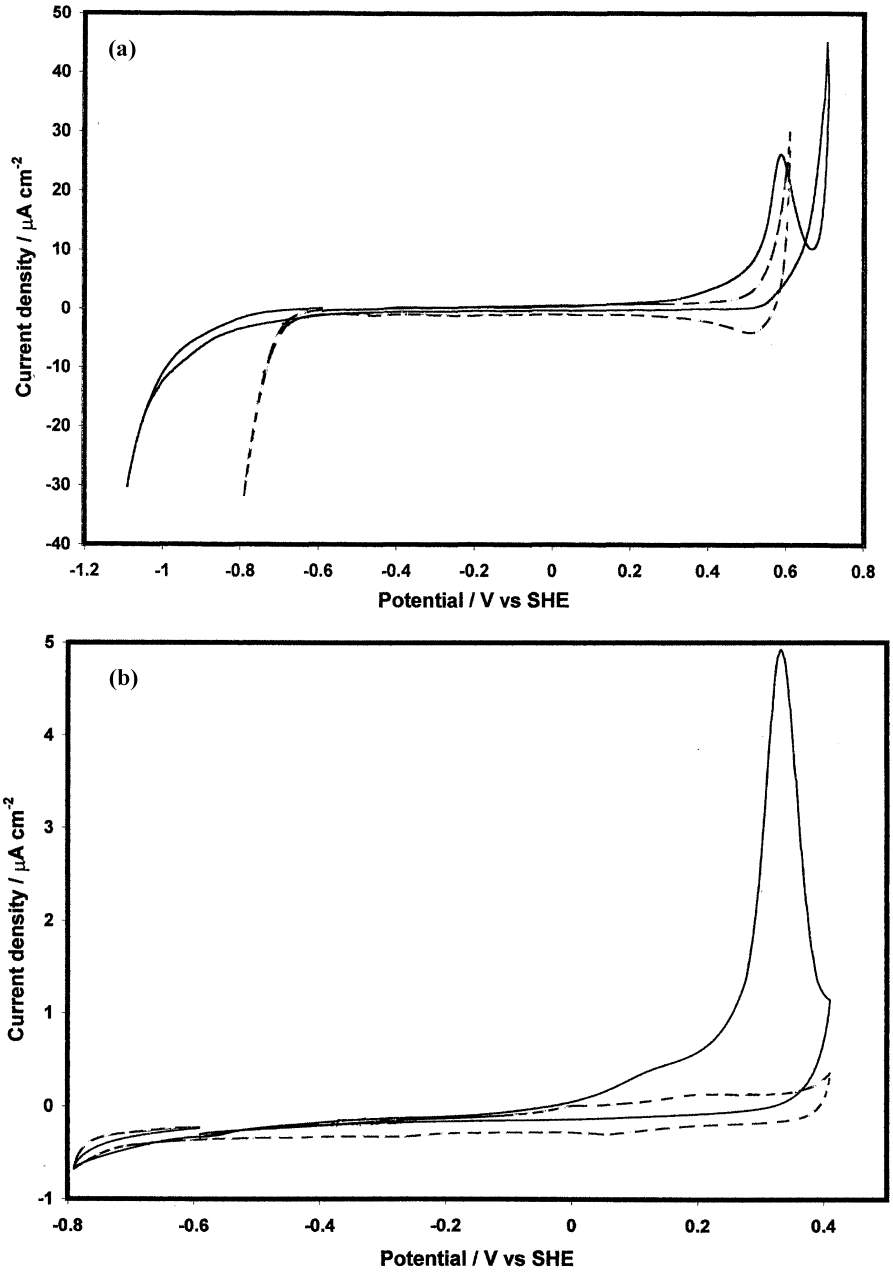

Fig. 4. Triangular potential sweep voltammograms for a silver electrode (a) at 5 mV s^{-1} in 0.05 mol dm^{-3} sodium tetraborate (pH 9.2) containing (– – –) 0 and (—) 10^{-3} mol dm^{-3} DIBDTPI and (b) at 0.5 mV s^{-1} in pH 11 buffer containing (- - -) 0 and (—) 10^{-3} mol dm^{-3} DIBDTPI.

In the presence of 10^{-3} mol dm^{-3} DIBDTPI, anodic current is observed at lower potentials; it commences at ~0.2 V and reaches a peak at ~0.6 V. This current flows in the potential region in which Basilio et al. [4] observed DIBDTPI-induced changes in IR intensity from a silver surface and hence can confidently be assigned to the formation of AgDIBDTPI.

Only a very small anodic current is apparent at potentials below 0.2 V in Figure 4(a) that could be identified with charge transfer adsorption of DIBDTPI. However, as pointed out in Section 3.1, negligible corrosion inhibition was observed on polarization curves at 5 mV s^{-1}, the scan rate used to record Figure 4(a). Thus, voltammograms were also recorded at the same scan rate as for the polarization curves in Figure 2 (i.e., 0.5 mV s^{-1}). The background electrolyte in this case was the same buffer of pH 11 as was used in the silver dissolution experiments. Figure 4(b) shows a voltammogram under these conditions and now an anodic current is apparent commencing at about −0.2 V and increasing at 0 V, the potentials at which Figure 2 shows inhibition of silver dissolution to be enhanced and the surface to begin to passivate, respectively. The current increases to a peak at ~0.34 V and this can be assigned to the formation of bulk AgDIBDTPI. The observed shift in the current peak with change in scan rate is symptomatic of a slow charge transfer process taking place. There is negligible cathodic current on the reverse scan at

potentials above about −0.4 V indicating that adsorption of DIBDTPI is electrochemically irreversible.

The integral anodic charge passed in the potential region −0.15 to 0.2 V, correcting for that passed in the buffer solution alone, is ~0.1 mC cm^{-2}. The charge associated with the chemisorption prewave observed for adsorption of a monolayer of ethyl xanthate on a silver surface treated in the same manner as in the present work was 75 μC cm^{-2}. Thus, the surface coverage of DIBDTPI at 0 V is about a monolayer. At higher potential, the bulk phase is formed:

$$Ag + DIBDTPI^- \rightarrow AgDIBDTPI + e^- \quad (3)$$

Further studies are being carried out to elucidate the interaction of DIBDTPI with copper, silver and gold surfaces under flotation-related conditions in the absence of cyanide.

4. Conclusions

(i) The presence of DIBDTPI inhibits both silver dissolution and oxygen reduction but the inhibition of these processes is significantly less than was reported previously [1] for 2-mercaptobenzothiazole.
(ii) The inhibition efficiency of 10^{-4} mol dm^{-3} DIBDTPI for silver dissolution in a pH 11 buffer solution containing 10^{-2} mol dm^{-3} CN^- was found to be 64.6%, and 95.0% over 10 min and 2 h, respectively.
(iii) The adsorption of DIBDTPI occurs by a slow charge transfer process at potentials significantly below where previous authors [4] have found Ag-DIBDTPI to be formed.
(iv) Adsorption of DIBDTPI displaces cyanide from the silver surface.

References

1. G.A. Hope, K. Watling and R. Woods, *J. Appl. Electrochem.* **31** (2001) 703.
2. J. Li and M.E. Wadsworth, *J. Electrochem. Soc.* **140** (1993) 1921.
3. S.S. Wang and P.V. Avotins, SME-AIME Annual Meeting, Dallas, Texas, 1982, Preprint 81-155, SME-AIME Littleton, CO (1982).
4. C.I. Basilio, D.S. Kim, R.H. Yoon, J.O. Leppinen and D.R. Nagaraj, SME Annual Meeting, Phoenix, AZ, 24–27 Feb. 1992, Preprint 92-174, SME-AIME Littleton, CO (1992).
5. R. Woods, G.A. Hope and K. Watling, *Minerals Eng.* **13** (2000) 345.
6. Dollish, Francis R., 'Characteristic Raman Frequencies of Organic Compounds,' (Wiley-Interscience, 1974).
7. R.P. Cooney, M.R. Mahoney and A.J. McQuillan, *Adv. Infrared Raman Spectrosc.* **9** (1982) 188.
8. R. Woods, G.A. Hope and K. Watling, *J. Appl. Electrochem.* **30** (2000) 1209.
9. R. Woods, G.A. Hope and G.M. Brown, *Colloids Surfaces A* **137** (1998) 329.
10. R. Woods, G.A. Hope and G.M. Brown, *Colloids Surfaces A* **137** (1998) 339.
11. R. Woods and G.A. Hope, *Colloids Surfaces A* **146** (1999) 63.
12. G.A. Hope, K. Watling and R. Woods, *Colloids Surfaces A* **178** (2001) 157.